DOI: 10.6060/tcct.20165912.5497

Для цитирования:
Лутовац М.В., Чуловская С.А., Кузьмин С.М., Парфенюк В.И. Влияние металла в структуре порфирина на кинетику электрополимеризации и морфологию пленок на основе гидроксифенилпорфирина. *Изв. вузов. Химия и хим. технология*. 2016. Т. 59. Вып. 12. С. 32–39.

For citation:
Lutovac M.V., Chulovskaya S.A., Kuzmin S.M., Parfenyuk V.I. Metal influence in porphyrine structure on kinetic of electrodeposition and morphology of hydroxyphenylporphyrins based films. *Izv. Vyssh. Uchebn. Zaved. Khim. Khim. Tekhnol.* 2016. V. 59. N 12. P. 32–39.

УДК: 547.979.7+544.023

М.В. Лутовац, С.А. Чуловская, С.М. Кузьмин, В.И. Парфенюк

Митар В. Лутовац

Факультет бизнеса и промышленного менеджмента, Университет «Унион», ул. Среднекраска, д. 4, Бараево, Белград, Сербия,11400
E-mail: lutovac@mail.ru

Светлана Альбертовна Чуловская (✉), Сергей Михайлович Кузьмин (✉), Владимир Иванович Парфенюк

Лаборатория «Новые материалы на основе макроциклических соединений», Институт химии растворов им. Г.А. Крестова РАН, ул. Академическая, 1, Иваново, Российская Федерация, 153045
E-mail: chulovskaya@yandex.ru (✉), smk@isc-ras.ru (✉), vip@isc-ras.ru

ВЛИЯНИЕ МЕТАЛЛА В СТРУКТУРЕ ПОРФИРИНА НА КИНЕТИКУ ЭЛЕКТРОПОЛИМЕРИЗАЦИИ И МОРФОЛОГИЮ ПЛЕНОК НА ОСНОВЕ ГИДРОКСИФЕНИЛПОРФИРИНА

Продемонстрирована принципиальная возможность получения пленок из ДМСО при активированном кислородом электрохимическом окислении гидроксифенилпорфирина и его цинкового комплекса. Изучена кинетика осаждения и морфология пленок. Показано, что происходит пассивация поверхности рабочего электрода при осаждении пленки порфирина-лиганда; при осаждении пленки металлокомплекса поверхность не пассивируется. Поэтому электрохимический метод позволяет сформировать достаточно толстые пленки с глобулярной структурой на базе металлокомплекса, и пленки малой толщины и слоистой структуры на базе порфирина-лиганда.

Ключевые слова: 2H-5,10,15,20-тетракис(4-гидроксифенил)порфирин, Zn-5,10,15,20-тетракис-(4-гидроксифенил)порфирин, электрополимеризация, морфология, кинетика

UDC: 547.979.7+544.023

M.V. Lutovac, S.A. Chulovskaya, S.M. Kuzmin, V.I. Parfenyuk

Mitar V. Lutovac

Faculty of Business and Industrial Management, University Union "Nikola Tesla", Belgrade, Serbia
E-mail: lutovac@mail.ru

Svetlana A. Chulovskaya, Sergey M. Kuzmin (✉), Vladimir I. Parfenyuk

Laboratory of New Materials on the Basis of Macrocyclic Compounds, G.A. Krestov Institute of Solution Chemistry of RAS, Akademicheskaya st., 1, Ivanovo, 153045, Russia
E-mail: chulovskaya@yandex.ru, smk@isc-ras.ru (✉), vip@isc-ras.ru

METAL INFLUENCE IN PORPHYRINE STRUCTURE ON KINETIC OF ELECTRODEPOSITION AND MORPHOLOGY OF HYDROXYPHENYLPORPHYRINS BASED FILMS

The films formation via activated by oxygen electrochemical oxidation of hydroxyphenylporphyrin and its zinc complex in dimethyl sulfoxide media was demonstrated. The different kinetics of deposition and morphologies of the films were observed. During the film deposition the working electrode surface was passivated in case of porphyrin-ligand, and was not passivated in case of metal complex. As a result, the electrochemical method leads to sufficiently thick films with a globular structure based on the metal complex and films o small thickness films and layered structure based on the porphyrin-ligand.

Key words: 2H-5,10,15,20-tetrakis(4-hydroxyphenyl)porphyrin, Zn-5,10,15,20-tetrakis(4-hydroxyphenyl)porphyrin, electropolymerization, morphology, kinetics

Porphyrin based film materials are promising as an effective catalysts [1, 2], an active elements of sensor devices [3, 4], in creating of organic transistors [5, 6], LEDs [7], nonlinear optical transmitters [8] and electrochromic devices [9, 10]. Their use as component of photovoltaic cells [11-13] is commercially attractive due to the ease of manufacturing technology, low cost, light weight, high efficiency at low light levels, possibility of manufacturing the flexible elements. There are several methods for film materials fabrication [14-16]. Formation of the film materials by electrochemical deposition makes it easy to control and adjust the film deposition process, as well as getting on a solid substrate (working electrode surface) of different types of materials [17, 18]. The proposed mechanism of the polyporphyrin films formation via electrochemical method is the recombination of the radical particles obtained after the porphyrin precursor oxidation [19-21]. Polymer hydroxyphenylporphyrin films or their metal complexes have been obtained previously in different media: aqueous solutions [22], dichloromethane [23], acetonitrile [24, 25]. Though, the influence of metal in the porphyrin cage on the film formation process was not sufficiently investigated yet.

In this paper polyporphyrin films obtained by activated electrochemical deposition. Formation of polyporphyrin films was performed from solutions 2H-5,10,15,20-tetrakis(4-hydroxyphenyl)porphyrin (H_2T(4OHPh)P) and Zn-5,10,15,20-tetrakis(4-hydroxyphenyl)porphyrin (ZnT(4OHPh)P) in dimethyl sulfoxide (DMSO). The formation and morphology kinetics of the films obtained on the basis of the porphyrin ligand and its metal complexes were compared.

EXPERIMENTAL

Procedure of synthesis

H_2T(4-OHPh)P was synthesized by the two-step method via demethylation of 2H-5,10,15,20-tetrakis(4-methoxyphenyl)porphirins [26, 27] obtained in high yield by condensation of benzaldehydes with pyrrole [28]. ZnT(4-OHPh)P was synthesized by refluxing of H_2T(4-OHPh)P in methanol with $Zn(OAc)_2$ excess for 3-4 hrs. The porphirins were purified by preparative column chromatography on aluminum oxide (Brockmann activity III). The purified products were studied by thin-layer chromatography (silufol plates), UV-VIS spectrometry (Varian Cary 50 spectrometer) and ^{1}H-NMR spectrometry (Bruker AVANCE-500 spectrometer) methods. The mass spectra were recorded on a Shimadzu Axima Confidence (MALDI-TOF) mass spectrometer. The products characteristics agree quite well with the reported data [29, 30]. The structures of porphyrins under study are shown in the Fig. 1.

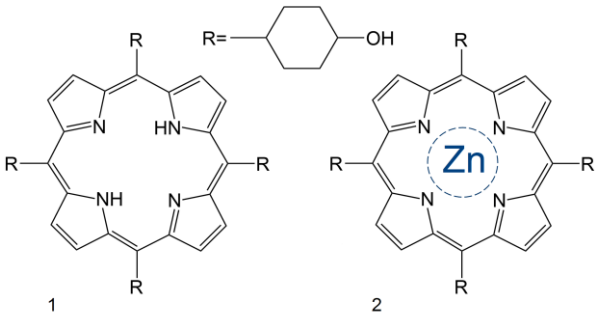

Fig. 1. Structural formulas of porphyrins under study
Схема 1. Структурные формулы изучаемых порфиринов

Electrochemical procedure

Dimethylsulfoxide (DMSO ≥ 99.5, ALDRICH) was purified by zone melting and then stored over molecular sieves in a dry box before use. Tetrabutylammonium perchlorate (TBAP ≥ 98.0, ALDRICH) was purified by recrystallization from ethanol. 10^{-3} M solutions of porphyrins containing 0.02 M TBAP as the supporting electrolyte were prepared by the gravimetric method using the electronic analytical balance «Sartorius» ME215S (the mass determination

error did not exceed 3%). A potentiostat SP-150 (Bio-Logic Science Instruments, France) was used for electrochemical measurements. The experiments were carried out in a three-electrode temperature-controlled (25±0.5 °C) electrochemical cell in freshly prepared solutions. The saturated calomel electrode (SCE) inserted into the electrochemical cell through the Luggin capillary was used as the reference electrode. The Pt wire was used as an auxiliary electrode.

As the working electrode, we used a polishing Pt strip (the working surface equaled 1.2 cm^2) rigidly fixed in the fluoroplastic lid. Before every measurement the active surface of the working electrode was mechanically mirror-polished, degreased with ethanol, etched with a chromic mixture for 20 min, carefully cleaned in distilled water and then in the solution under study. The working electrode was immersed in the cell with the test solution where the potential of the working electrode reached a steady value over 10 min. In order to degas or oxygenate solutions before the electrochemical measurements, argon or oxygen was bubbled through the capillary tube for 30 min. In earlier paper we have shown that in DMSO media the more effective electrochemical deposition of polyporphyrin films was obtained under activation by oxygen [31, 32]. Therefore, in this paper the polyporphyrin films deposition included cycling of the working electrode potential in the oxygenated solutions (to activate the deposition process), then cycling in degassed solutions (to stabilize the resulting film). The deposition process consisted of three stages. Each stage consisted of 10 cycles in the degassed solution and 10 cycles in an oxygenated solution. CV response was recorded at scan rate of 0.02 V/s. The CV data were corrected for Ohmic (iR) losses using the current interruption technique [33].

Electrochemical impedance spectroscopy (EIS) measurements during of polyporphyrin films formation were performed using Solartron SI 1260 analyzer at frequency range from 10^{-1} to 10^6 Hz with sinusoidal excitation voltage of 10 mV. We use two-electrode cell for EIS study. The working and auxiliary electrodes were placed at 5 mm opposite to each other. Face of polished Pt wire diameter of 2.5 mm, pressed in teflon sleeve was used as working electrode. Platinized platinum disc 25 mm in diameter was used as auxiliary electrode. Electrochemical cell was connected to the measuring device by two-electrode four-wire scheme to avoid an effect of current-carrying wires. Analysis of EIS data was performed using ZView2 program. Atomic force microscope (AFM) images were obtained using the Solver-47-Pro equipment and processed by a Nova RC software.

RESULTS AND DISCUSSION

Fig. 2 shows cyclic voltammograms obtained at polyporphyrin films deposition from DMSO solutions.

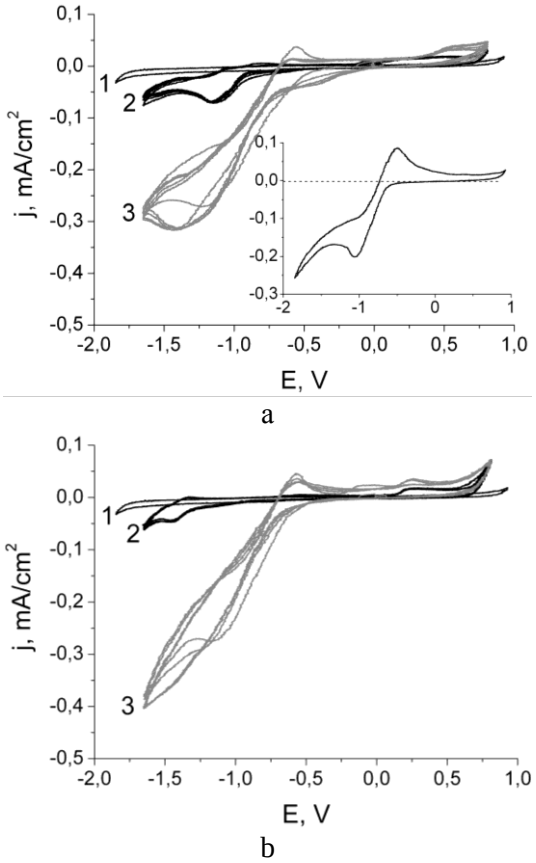

Fig. 2. The electrochemical response of H_2T(4-OHPh)P (a) and ZnT(4-OHPh)P (b) solutions during potential cycling. Scan rate - 0.02 V/s. 1 - background current; 2 - degassed porphyrin solution; 3 - oxygenated porphyrin solution. The inset shows the oxygen electrochemical response in DMSO without porphyrin

Рис. 2. Электрохимический отклик растворов H_2T(4-OHPh)P (a) и ZnT(4-OHPh)P (b) при циклировании потенциала. Скорость развертки потенциала 0.02 В/с. 1 – фоновый ток; 2 – дегазированный раствор порфирина; 3 - насыщенный кислородом раствора порфирина. На вставке представлен электрохимический отклик кислорода в ДМСО при отсутствии порфирина

Degassed solutions CV response (Fig. 2 a, b, curve 2) shows low-intensive wide irreversible oxidation peaks at the potentials more than +0.12 V for the porphyrin ligand and +0.17 V for the metal complex and irreversible reduction peaks with half-wave potential of -1.03 for H_2T(4OHPh)P) and -1.35 V for ZnT (4OHPh)P. The irreversibility of the electrochemical peaks of porphyrins associated with the intramolecular electron transfer following the oxidation or reduction processes [34, 35]. The CV shape is slightly varied from cycle to cycle for the degassed solutions. Oxygenated solutions of porphyrins CV

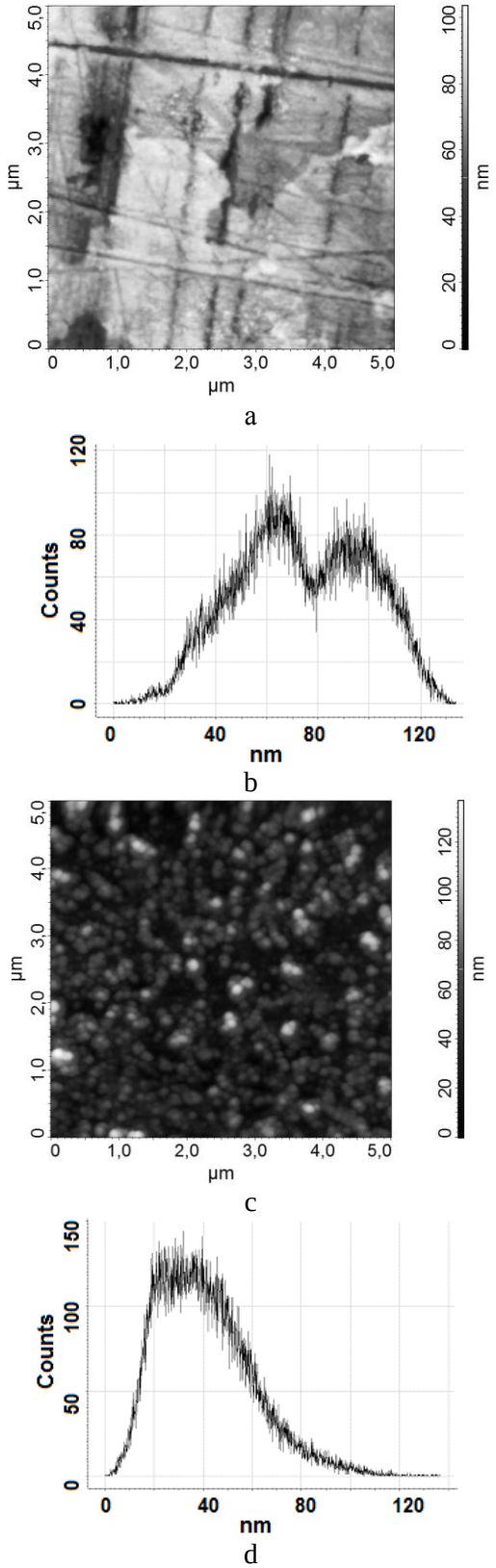

Fig. 3. AFM images of polyporphyrin films (H_2T(4OHPh)P (a), ZnT(4OHPh)P (c)) and histograms of heights (inset) of H_2T(4OHPh)P (b) and ZnT(4OHPh)P (d)

Рис. 3. АСМ-изображения пленок поли-H_2T(4OHPh)P (a), поли- ZnT(4OHPh)P (c) и гистограммы высот пленок поли-H_2T(4OHPh)P(b), поли- ZnT(4OHPh)P (d)

response (Fig. 2 a, b, curve 3) shows intense irreversible peak of oxygen electroreduction at potentials more negative than -0.5 V. In the absence of porphyrins the electroreduction of oxygen in DMSO is quasi reversible (inset in Fig. 2a) and leads to superoxide anion radicals formation through the one-electron mechanism: ($O_2^{\bullet-}$): $O_2 + e \rightarrow O_2^{\bullet-}$ [36-39]. At the porphyrins presence the electroreduction of oxygen turn to irreversibility due to an effective interaction of superoxide with porphyrins [40-43]. Additionally CV shape of oxygenated porphyrins solutions is significantly changed from cycle to cycle. The gradual change in CV curves was accompanied with the polyporphyrin film formation on the surface of the working electrode. The resulting film has a golden color and is insoluble in water, alcohol, dichloromethane.

According to AFM images the obtained poly-H_2T(4OHPh)P and poly ZnT(4OHPh)P films has different morphology (Fig. 3). In the case of poly-H_2T(4OHPh)P (Fig. 3a) there are micro-scratches, typical for polished Pt electrode that indicates a small thickness of the film. The observed growth steps and a histogram of heights with two maximums (Fig. 3b) let us to conclude layered structure of poly-H_2T(4OHPh)P film. Unlike poly-ZnT(4OHPh)P films the structure of the particles forming the poly-H_2T (4OHPh)P films can not be discern at Solver-47- Pro resolution. ZnT(4OHPh)P surface (Fig. 3c) is formed of round globules with a lateral size of 40-100 nm. The globular structure of the film leads to a heights histogram with a single maximum (Fig. 3d). The substrate microroughnesses can not be seen on the AFM image, due to the large thickness of the films.

EIS study of polyporphyrin films formation was performed in aerated solutions for the stationary potential of the working electrode. The deposition potential had been determined by a preliminary experiment. For this purpose obtained at different potentials of the working electrode EIS data were modeled by Randles-Ershler scheme (Fig. 4) [44]. The calculated polarization resistance values reached a minimum at potential about +0.95 V for H_2T(4OHPh)P and about +0.8 V for ZnT(4OHPh)P vs Pt quasireference electrode. These potentials were used at studying of the films formation kinetics via impedance monitoring during the process (Fig. 4) [45].

It is clear to see the difference in Nyquist plots of H_2T(4OHPh)P and ZnT(4OHPh)P during the whole experiment. In case of H_2T(4OHPh)P the Nyquist plots generally are elements of the circle, that allows to suggest a minor contribution of diffusion limitations in the electrode process. In case of ZnT(4OHPh)P elements of the circles come to a slop

lines at frequencies ~1.5 Hz which indicates mixed kinetic-diffusion control. Comparison of process parameters was carried out using Randles-Ershler equivalent circuit. Equivalent circuit included resistance of the solution Rs, the polarization resistance Rp, Warburg element W and an element of constant phase Q (Fig. 4). Elements W and Q are elements with distributed parameters and are determined by several characteristics.

$$\text{Element} \quad Q: \; Q = \frac{1}{A \cdot (i\omega)^n} \qquad (1)$$

where A – independent of frequency pre-exponential factor; n – index extent determined with the nature of the frequency dependence (1 < n < -1) i – imaginary unit; ω = 2πf – circular frequency. Element Q is capacitive type for n close to 1 and one is diffusion type for n close to n 0,5.

$$\text{Warburg element:} \; W = \frac{W_R \cdot \tanh(iB\omega)^p}{(iB\omega)^p}, \qquad (2)$$

where W_R – diffusion mass transfer resistance; B – characteristic time of diffusion transfer; p – the dimensionless exponent which can take values from 0 to 1.

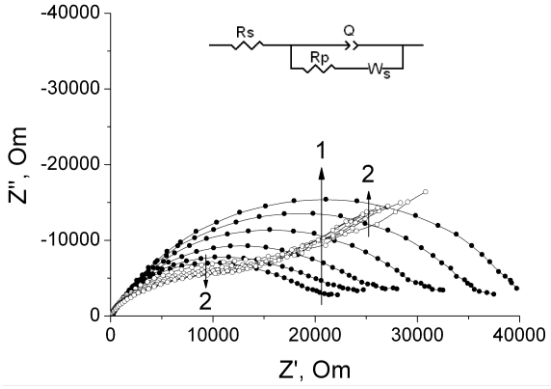

Fig. 4. Nyquist plots changing for $H_2T(4OHPh)P$ (•) and ZnT(4OHPh)P (o) films deposition. The time points are 10, 20, 30, 40, 50 and 60 min, the arrows 1- ($H_2T(4OHPh)P$) and 2- (ZnT(4OHPh)P) show the directions of plots displacement over time
Рис. 4. Изменение диаграммы Найквиста при осаждении пленок $H_2T(4OHPh)P$ (o, 1), ZnT(4OHPh)P (•, 2). Моменты времени 10, 20, 30, 40, 50 и 60 мин. Стрелками указаны направления смещения годографов с течением времени

High precision of fitting of EIS data and small quantity of statistical criterion χ^2 (about 10^{-4}) provides the accuracy of applied model.

The obtained at the fitting values n of the Q element are in the range of 0.73 to 0.81 for $H_2T(4OHPh)P$ and ZnT(4OHPh)P. It points to the capacitive type of interphase boundary and allows to calculate the "true capacitance" (C) of the interface by the ratio of (3) [46]:

$$C = (A \cdot R_p)^{1/n}/R_p \qquad (3)$$

Results of fitting and calculations are presented in Table.

Table 1

Model characteristics of impedance at different times of deposition of $H_2T(4OHPh)P$ and ZnT(4OHPh)P films on Pt electrode

***Таблица.* Характеристики импеданса при различных временах осаждения $H_2T(4OHPh)P$ и ZnT(4OHPh)P на Pt электроде**

Time, min	A·10^6	n	R_p, Om	W_R, Ом	B, c	p	C, μF
$H_2T(4OHPh)P$)							
5	2.62	0.81	16973	5079	5.53	0.38	1.28
10	2.82	0.80	18474	7493	7.68	0.34	1.32
15	2.74	0.80	19023	9743	11.11	0.32	1.28
20	2.75	0.79	21005	7412	5.13	0.40	1.28
30	2.52	0.78	25846	4758	3.38	0.54	1.17
40	2.24	0.78	31732	2426	2.71	0.68	1.06
50	2.05	0.78	37231	733	2.18	0.83	1.00
60	1.92	0.79	41843	324	2.56	0.91	0.97
ZnT(4OHPh)P							
5	2.65	0.78	12244	63173	17.31	0.39	1.03
10	2.39	0.80	13155	82876	28.97	0.41	1.01
15	2.85	0.78	12418	68663	20.66	0.41	1.09
20	3.02	0.77	12039	67302	21.22	0.41	1.12
30	3.44	0.75	12214	58476	16.11	0.43	1.20
40	3.68	0.74	11821	56632	15.89	0.43	1.25
50	4.07	0.73	11663	53251	14.84	0.43	1.32
60	4.15	0.73	11128	51453	14.60	0.43	1.32

The data analysis shows a slight effect of diffusion on the electrode process (WR << Rp) for $H_2T(4OHPh)P$. It leads to low accuracy of the calculated diffusion characteristics in the case of $H_2T(4OHPh)P$ and does not allow us to compare the diffusion behavior of $H_2T(4OHPh)P$ and ZnT(4OHPh)P.

Parameter R_p characterizes the rate of electron transfer at interface and it was close for both studied porphyrins for the initial time. There are no significant changes in this parameter over time for ZnT(4OHPh)P. Since the formation of the poly-ZnT(4OHPh)P film in the experiment is confirmed, it means a high probability of charge transfer through the deposited layer and sufficient conductivity of the film forming. In contrast to poly-ZnT(4OHPh)P film formation the Rp parameter increases by 2.5 times during the experiment for $H_2T(4OHPh)P$. This change in polarization resistance clearly points to the passivation of the working electrode surface as a result of the formation of the poly-$H_2T(4OHPh)P$ surface film. Apparently, the surface passivation is a reason of thinness of $H_2T(4OHPh)P$ film that could be seen at AFM (Fig. 3).

The “true capacitance” value extrapolates the interface properties to the ideal plane capacitor prop-

erties. Parameter C depends on the plate area (area of contact between the phases varied due to changing in the morphology of the surface layer) and distance between opposite charges (the distribution of charges in the interfacial layer). According to Table in the case of poly-H_2T(4OHPh)P film formation "true capacitance" is close to a constant value during the 20 min, then decreases. In the case of poly- ZnT(4OHPh)P film formation "true capacitance" is constant initially, close to a constant value during the 10 min, then increases. The set of parameters changes over time indicates film formation staging for the both porphyrins. The decreasing in "true capacitance" in the case H_2T(4OHPh)P may be explained by poorly conducting surface film forming which increases the distance between free charges in interfacial double layer. The capacity increasing in the case ZnT(4OHPh)P indicates an increasing in the specific electrode surface area during the film formation. Thus, in the case of poly-ZnT(4OHPh)P film growth the "true capacitance" values indicate extended surface of interfacial boundary forming. The parameter n can be interpreted in term of fractal dimension of electrode surface [47, 48]. Decreasing in n during the film deposition indicates fractal dimension increasing and formation of a more extended surface also.

CONCLUSION

We have shown the ability of obtain the electrochemically deposited poly-hydroxyphenylporphyrin films in DMSO media. On the one hand, the increasing in solvents number allows improving the variability of electrochemical method. On the other hand, DMSO solution has low toxicity that leads to safe practice of films deposition. Films were formed via activated by dissolved oxygen electrochemical oxidation of 5,10,15,20-tetrakis(4-hydroxyphenyl)-porphyrin and its Zn complex. The influence of metal atom in the macrocycle cage on deposition kinetics and properties of the resulting film was demonstrated. It was found in the case of H_2T(4OHPh)P the electrode surface is passivated while film formation that leads to small thickness and a layered structure. At the electrochemical deposition of polymer films ZnT(4OHPh)P the surface is not passivated and it allows to obtain sufficiently thick films with a globular structure.

Acknowledgements

The authors thank the upper Volga region centre of physic-chemical research (G.A. Krestov Institute of Solution Chemistry of the Russian Academy of Sciences) for technical support, the Russian Foundation for Basic Research research (grant 15-43-03006) for partial financial support.

REFERENCES

1. **Chehg N., Kemna C., Goubert-Renaudin S., Wieckowski A.** Reduction reaction by porphyrin-based catalysts for fuel cells. *Electrocatal.* 2012. V. 3. P. 238-251.
2. **Hod I, Sampson M.D., Deria P., Kubiak C.P., Farha O.K., Hupp J.T.** Fe-porphyrin-based metal–organic framework films as high-surface concentration, heterogeneous catalysts for electrochemical reduction of CO2. *ACS Catal.* 2015. V. 5. P. 6302-6309.
3. **Paske A.C., Gunsch M.J., O'Donnell J.L.** Electropolymerized Ultrathin Chromophore Films for VOC Sensing. *ECS Transactions.* 2011. V. 35. P. 29-34.
4. **Lvova L., Natale C.D., Paolesse R.** Porphyrin-based chemical sensors and multisensor arrays operating in the liquid phase. *Sensors and Actuators B.* 2013. V. 179. P. 21-31.
5. **Khaderbad M.A., Tjoa V., Rao M., Phandripande R., Madhu S., Wei J., Ravikanth M., Mathews N., Mhaisalkar S.G., Rao V.R.** Fabrication of unipolar graphene field-effect transistors by modifying source and drain electrode interfaces with zinc porphyrin. *ACS Appl. Mater. Interfaces.* 2012. V. 4. P. 1434-1439. DOI: 10.1021/am201691s.
6. **Hoang M.H., Choi D.H., Lee S.J.** Organic field-effect transistors based on semiconducting porphyrin single crystals. *Synthetic Metals.* 2012. V. 162. P. 419-425. DOI: 10.1016/j.synthmet.2012.01.005.
7. **Zhou J., Liu Q., Feng W., Sun Y., Li F.** Upconversion luminescent materials: advances and applications. *Chem. Rev.* 2015. V. 115. P. 395-465. DOI: 10.1021/cr400478f.
8. **El-Nahass M.M., Farag A.A.M., El-Metwally M., Abu-Samaha F.S.H., Elesh E.** Structural, absorption and dispersion characteristics of nanocrystalline copper tetraphenyl porphyrin thin films. *Synthetic Metals.* 2014. V. 195. P. 110-116. DOI: 10.1016/j.synthmet.2014.05.013.
9. **Gervaldo M., Funes M., Durantini J., Fernandez L., Fungo F., Otero L.** Electrochemical polymerization of palladium (II) and free base 5,10,15,20-tetrakis(4-N,N-diphenylaminophenyl)porphyrins: Its applications as electrochromic and photoelectric materials. *Electrochimica Acta.* 2010. V. 55. P. 1948-1957. DOI: 10.1016/j.electacta.2009.11.014.
10. **Durantini J., Morales G.M., Santo M., Funes M., Durantini E.N., Fungo F., Dittrich T., Otero L., Gervaldo M.** Synthesis and characterization of porphyrin electrochromic and photovoltaic electropolymers. *Organic Electronics.* 2012. V. 13. P. 604-614. DOI: 10.1016/j.orgel.2012.01.004.
11. Solar Cells - Dye-Sensitized Devices. Ed. Prof. Kosyachenko L.A. In Tech. 2011. 492 p.
12. **Suarez M.B., Durantini J., Otero L., Dittrich T., Santo M., Milanesio M.E., Durantini E., Gervaldo M.** Electrochemical Generation of Porphyrin-Porphyrin and Porphyrin-C60 Polymeric Photoactive Organic Heterojunctions. *Electrochimica Acta.* 2014. V. 133. P. 399-406. DOI: 10.1016/j.electacta.2014.04.011.
13. **Day N.U., Wamser C.C., Walter M.G.** Porphyrin polymers and organic frameworks. *Polym. Int.* 2015. V. 64. P. 833-857. DOI: 10.1002/pi.4908.
14. **Drain C.M., Varotto A., Radivojevic I.** Self-organized porphyrinic materials. *Chem. Rev.* 2009. V. 109. P. 1630-1658. DOI: 10.1021/cr8002483.
15. **Pop S.D., Kate S.P., Rappich J., Hinrichs K.** Tunable optical constants of thermally grown thin porphyrin films on silicon for

photovoltaic applications. *Solar Energy Materials & Solar Cells.* 2014. V. 127. P. 169-173. DOI: 10.1016/j.solmat.2014.04.032.

16. **Giancane G., Valli L.** State of art in porphyrin langmuir-blodgett films as chemical sensors. *Advances in Colloid and Interface Science.* 2012. V. 171–172. P. 17-35. DOI: 10.1016/j.cis.2012.01.001.
17. **Yoshida T., Zhang J., Komatsu D., Sawatani S., Minoura H., Pauporte T., Lincot D., Oekermann T., Schlettwein D., Tada H., Wohrle D., Funabiki K., Matsui M., Miura H., Yana H.** Electrodeposition of inorganic/organic hybrid thin films. *Adv. Funct. Mater.* 2009. V. 19. P. 17–43. DOI: 10.1002/adfm.200700188.
18. Modern Electroplating. Schlesinger M., Paunovic M. (Eds). John Wiley & Sons, Inc. 2010. 736 p.
19. **Bettelheim A., White B.A., Raybuck S.A., Murray R.W.** Electrochemical polymerization of amino-, pyrrole-, and hydroxy-substituted tetraphenylporphyrins. *Inorg. Chem.* 1987. V. 26. P. 1009-1017. DOI: 10.1021/ic00254a011.
20. **Walter M.G., Wamser C.C.** Synthesis and characterization of electropolymerized nanostructured aminophenylporphyrin films. *J. Phys. Chem. C.* 2010. V. 114. P. 7563-7574. DOI: 10.1021/jp910016h.
21. **Durantini J., Otero L., Funes M., Durantini E.N., Fungo F., Gervaldo M.** Electrochemical oxidation-induced polymerization of 5,10,15,20-tetrakis[3-(N-ethylcarbazoyl)]porphyrin (P-CBZ). Formation and characterization of a novel electroactive porphyrin thin film. *Electrochimica Acta.* 2011. V. 56. P. 4126-4134. DOI: 10.1016/j.electacta.2011.01.111.
22. **Hrbáč J., Gregor Č., Machová M., Králová J., Bystroň T., Číž M., Lojek A.** Nitric oxide sensor based on carbon fiber covered with nickel porphyrin layer deposited using optimized electropolymerization procedure. *Bioelectrochemistry.* 2007. V. 71. P. 46. DOI: 10.1016/j.bioelechem.2006.09.007.
23. **Murugan A., Nagarajan E.R., Manohar A., Kulandaisamy A., Lemtur A., Muthulaksmi L.** Synthesis and electrochemical studies on oxidative products of vanadyl meso-5,10,15,20-tetrakis(p- hydroxyphenyl)porphyrin. *Int. J. Chem. Tech.* 2013. V. 5. P. 1646.
24. **Humphrey J., Kuciauskas D.** Charge-transfer states determine iron porphyrin film third-order nonlinear optical properties in the near-ir spectral region. *J. Phys. Chem. B.* 2004. V. 108. P. 12016. DOI: 10.1021/jp0485643.
25. **Quan Y., Xue Z., Wu B., Qi H., Liu D.** Determination of explosives based on novel type of sensor using porphyrin functionalized carbon nanotubes. *Colloids and Surfaces B: Biointerfaces.* 2011. V. 88. P. 396. DOI: 10.1016/j.colsurfb.2011.07.020.
26. **Milgrom L.R.** Synthesis of some new tetra-arylporphyrins for studies in solar energy conversion *J. Chem. Soc., Perkin Trans. I.* 1983. P. 2535-2539. DOI: 10.1039/p19830002535.
27. **Syrbu S.A., Semeykin A.S.** Synthesis of (hydroxyphenyl)porphyrins. *Zhurn. Org. Khim.* 1999. V. 35. P. 1262-1265 (in Russian).
28. **Semeikin A.S., Koifman O.I., Berezin B.D.** Improved method for synthesis of substituted tetraphenylporphins. *Chemistry of Heterocyclic Compounds.* 1986. V. 22. P. 629-632. DOI: 10.1007/BF00575244.
29. **Rumyantseva V.D., Gorshkova A.S., Mironov A.F.** Improved Method of 5,10,15,20-Tetrakis(4-hydroxyphenyl)-porphyrins Synthesis. *Macroheterocycles.* 2013. V. 6. P. 59-61. DOI: 10.6060/mhc130222r.
30. **Rojkiewicz M., Kus P., Kozub P., Kempa M.** The synthesis of new potential photosensitizers [1]. Part 2. Tetrakis-(hydroxyphenyl)porphyrins with long alkyl chain in the molecule. *Dyes and Pigments.* 2013. V. 99. P. 627-635. DOI: 10.1016/j.dyepig.2013.06.029.
31. **Chulovskaya S.A., Kuzmin S.M., Parfenyuk V.I.** poly-aminophenylporfirin film formation activated by superoxide anion radicals. *Macroheterocycles.* 2015. V. 8. P. 259-265. DOI: 10.6060/mhc150662k.
32. **Chulovskaya S.A., Kuzmin S.M., Shilov A.N., Parfenyuk V.I.** Synthesis and property of semiconductor films of poly-5,10,15,20-tetrakis (4'-aminophenyl) porphyrin. *Perspektivnyye materialy.* 2016. N 5. P. 33-40 (in Russian).
33. **Taylor S.R., Scribner L.L.** The measurement and correction of electrolyte resistance in electrochemical tests. Philadelphia: American Society for Testing and Materials. 1990.
34. **Morehouse K.M., Sipe H.J.JR, Mason R.P.** The one-electron oxidation of porphyrins to porphyrin pi-cation radicals by peroxidases: An electron spin resonance investigation. *Archives of biochemistry and biophysics.* 1989. V. 273. P. 158-164.
35. **Zhu W., Sintic M., Ou Z., Sintic P.J., McDonald J.A., Brotherhood P.R., Crossley M.J., Kadish K.M.** Electrochemistry and spectroelectrochemistry of β,β′-fused quinoxalinoporphyrins and related extended bis-porphyrins with Co(III), Co(II), and Co(I) central metal ions. *Inorg Chem.* 2010. V. 49. P. 1027-1038. DOI: 10.1021/ic901851u.
36. **Sawyer D.T., Roberts J.L.J.** Electrochemistry of oxygen and superoxide ion in dimethylsulfoxide at platinum, gold and mercury electrodes. *Electroanal. Chem.* 1966. N 12. P. 90-101.
37. **Fujinaga T., Isutsy K., Adachi T.** Polarographic studies of dissolved oxygen in dimethylsulphoxide–water mixtures. *Bull. Chem. Soc. Jap.* 1969. V. 42. P. 140-145. DOI: 10.1246/bcsj.42.140.
38. **Islam M.M., Okajima T., Ohsaka T.** In situ CCD video and voltammetric studies on enhanced cathodic peak observed at a hanging mercury drop electrode during consecutive two one-electron redox reactions in aprotic solutions. *J. Electroanal. Chem.* 2008. V. 618. P. 1–10. DOI: 10.1016/j.jelechem.2008.02.013.
39. **Laoire C.O., Mukerjee S., Abraham K.M., Plichta E.J., Hendrickson M.A.** Influence of nonaqueous solvents on the electrochemistry of oxygen in the rechargeable lithium−air battery. *J. Phys. Chem.* 2010. V. 114. P. 9178-9186. DOI: 10.1021/jp102019y.
40. **Kuzmin S.M., Chulovskaya S.A., Parfenyuk V.I.** Estimation of antioxidant activity of tetrakis(p–aminophenyl)- porphine regard to superoxide ions by voltammetry method. *Macroheterocycles.* 2013. V. 6. P. 334-339. DOI: 10.6060/mhc131057k.
41. **Kuzmin S.M., Chulovskaya S.A., Parfenyuk V.I.** Substituent position influence on the electrochemical properties and antioxidant activity of tetra(aminophenyl)porphyrins. *J. Porphyrins Phthalocyanines.* 2014. V. 18. P. 585-593. DOI: 10.1142/S108842461450031X.
42. **Kuzmin S.M., Chulovskaya S.A., Parfenyuk V.I.** The coulometric approach to the superoxide scavenging activity determination: the case of porphyrin derivatives influence on oxygen electroreduction. *J. Porphyrins Phthalocyanines.* 2015. V. 19. P. 1053–1062. DOI: 10.1142/S1088424615500807.

43. **Kuzmin S.M., Chulovskaya S.A., Parfenyuk V.I.** Mechanism and superoxide scavenging activity of hydroxy substituted tetraphenylporphyrins via coulometric approach. *J. Electroanal.Chem.* 2016. V. 772. P. 80-88. DOI: 10.1016/j.jelechem.2016.04.024.
44. **Sluyters-Rehbach M.** Physical and biophysical chemistry division commission on electrochemistry. *Pure Appl. Chem.* 1994. V. 66. P. 1831.
45. **Kuz'min S.M., Chulovskaya S.A., Parfenyuk V.I.** Effect of anodic potential on process of formation of polyporphyrin film in solutions of tetrakis(p-aminophenyl)porphin in dichloromethane. *Russ. J. Electrochem.* 2014. V. 50. P. 429–437. DOI: 10.1134/S1023193514050073.
46. **Jovic V.D., Jovic B.M.** EIS and differential capacitance measurements onto single crystal faces in different solutions: Part I: Ag(111) in 0.01 M NaCl. *J. Electroanal. Chem*. 2003. V. 541. P. 1-11. DOI: 10.1016/S0022-0728(02)01309-8.
47. **Nyikos L., Pajkossy T.** Fractal dimension and fractional power frequency-dependent impedance of blocking electrodes. *Electrochem. Acta*. 1985. V. 30. P. 1533-1540. DOI: 10.1016/0013-4686(85)80016-5.
48. **Liu S.H.** Fractal model for the ac response of a rough interface. *Phys. Rev. Lett.* 1985. V. 55. P. 529-532. DOI: 10.1103/PhysRevLett.55.529.

Поступила в редакцию 28.09.2016
Принята к опубликованию 07.11.2016

Received 28.09.2016
Accepted 07.11.2016